nature portfolio

Peer Review File

Deuteration-enhanced neutron contrasts to probe amorphous domain sizes in organic photovoltaic bulk heterojunction films

REVIEWER COMMENTS

Reviewer #1 (Remarks to the Author):

Cai et. al. used isotrope labeling method to measure the amorphous domain size of deuterated Y6 molecules in the blend film of PM6:d-Y6 and experimentally uncovered a structure-property relationship between the short-range aggregation of Y6 molecules and the performance of OPV devices. The authors combined GISAXS and GISANS techniques to evaluate the scattering length densities of polymeric donners and acceptors, which give a large contrast to distinguish the aggregation of acceptors. Although GISANS has been widely utilized in OPV studies (refs. 28-33), the aggregation nature of Y6 in amorphous domains is significant to understanding the role of Y6, as an emerging acceptor, in the development of high-performance solar cells. Thus, I recommend this work to publish in nature communication after the response to the following comments:

1) All the data in this manuscript are obtained by GISAXS and GISANS. Although these two techniques are powerful to support the conclusion, would the authors additionally provide AFM phase images to observe and evaluate the phase separation of PM6:d-Y6? To do so, the crystalline and amorphous domain sizes could be measured directly.

2) The authors fitted the GISAXS and GISANS intensity profile using equation 1, and provided the information of nanomorphology in PM6:d-Y6 film. In line 226-227, they claim that GISAXS profile gave "the correlation length (ξ) of the amorphous intermixing phase and the size of the crystalline acceptor domain." In my opinions, both the PM6 and d-Y6 are crystalline in the blend films, so why only crystalline domain of Y6 acceptor can be evaluated by fitting the equation?

3) Would the authors explain the reason to choose a PM6:Y6 BHJ blend as the active layers in OPV devices instead of PM6:d-Y6? Since all the information on the nanomorphology of blend films comes from PM6:d-Y6, the corresponding devices are better to be tested for data consistency, although the performance of two devices comprising PM6:Y6 and PM6:d-Y6 may be identical (as shown in Fig. S8b)

Others:

4) line 57, the "research" should be plural so "has" is used wrongly in grammar.

5) line 91, the "challenghg" is a typo.

6) line 103, "not" in the term of "it originates not from crystalline phases..." is inappropriately expressed in grammar.

7) line 129, the "aggregation" should be singular.

8) line 137, "Supplementary Fig. 6" should be "Supplementary Fig. 7".

9) line 202, the correspondence of fig. 3a and 3b to GISANS and GISAXS is an error.

Reviewer #2 (Remarks to the Author):

The main novelty of this work is that the authors deuterated the non-fullerene acceptor (NFA) Y6 to overcome the lack of neutron contrast in OPV films based on NFAs. This allowed them to study the nano-morphology of the OPV films using GISANS. This work is merely incremental, and it lacks the originality needed to be published in this journal.

In the abstract the authors say that their work uncovers "for the first time" the amorphous nanomorphology of OPV films. This is not correct – this has been addressed before either using neutron scattering or Resonant Soft X-ray Scattering (RSoXS) techniques.

Neutron scattering (SANS and Neutron reflectivity) have been previously used extensively to study fullerene-based OPVs and the authors are advised to improve their literature survey and include some important references that are missing. For example, these below among many others.

Wienhold, K.S., “Organic solar cells probed with advanced neutron scattering techniques” Applied Physics Letters, 116, 120504 (2020)

Zhang, Y. et al, "Understanding and controlling morphology evolution via DIO plasticization in PffBT4T-2OD/PC71BM devices", Scientific Reports 7, 44269 (2017)

Chen D. “P3HT/PCBM Bulk Heterojunction Organic Photovoltaics: Correlating Efficiency and Morphology”, Nano Lett. 2011, 11, 2, 561–567

Bernardo, G. et al "Impact of 1,8-diiodooctane on the morphology of organic photovoltaic (OPV) devices – A Small Angle Neutron Scattering (SANS) study", Polymer Testing 82 (2020) 106305

Reviewer #3 (Remarks to the Author):

The authors used a combination of neutron scattering - in terms of GISANS technique - and deuteration to probe the nanomorphology of the PM6:d-Y6 blend film. The deuteration was selectively done for the NFA Y6 (d-Y6). The measurements were underpinned by MD calculations. The study highlighted a specific short-range aggregation of Y6 - as an intrinsic feature of this NFA, that was concluded to be a key contributor to the high photovoltaic performance of most Y6-containing organic bulk heterojunction systems. Indeed, the authors studied other polymers than PM6, and have supported the neutron data by measurements using different x-ray and light-based techniques.

The manuscript is dense, organized and well written. The topic, techniques and findings warrant publication in Nature Communications after considering the following comment.

The only concern readers, who might be interested in applying neutron scattering and associated deuteration in their research on OPVs, would be to have some more targeted references on the application of neutron scattering and deuteration to study morphology and local properties, including

dynamics, beyond GISANS by including other neutron-based techniques. In this context, the authors are invited to enrich the introduction and the reference list by considering recent works on binary and ternary blend, either with acceptors being fullerenes (PCBM, etc) or NFAs (O-IDTBR, etc).

Reviewer #4 (Remarks to the Author):

Deuteration-enhanced neutron is cleverly applied to GISANS test, and the unique short-range aggregation behavior of Y6 in the D/A blending region is effectively detected, which also confirms the experimental results of other research groups. Prof Lu and co-workers provide a novel method for detecting the aggregate state of non-crystalline domain in active layer of OSCs. However, SANS is already a conventional and mature characterization technique, and deuterated materials have also been applied to SANS. In addition, the PM6:Y6 device in the paper is a very conventional, although the authors claim that directionally deuterated SANS technology offers opportunities for complex active layer systems and intermolecular interaction mechanisms. The innovation of this article is insufficient. The authors did not validate the proposed large short-range aggregation of acceptors in the D/A blend region as a key to recent high-performance organic solar cells and provide insights for improving the efficiency or stability of organic solar cells, so it is not recommended for publication in Nature Communication.

1. Prof. Ye has demonstrated that deuterated solvents can improve the performance of organic solar cells (Aggregate 2023, 4, e289). d-Y6 shows similar photoelectric properties to Y6 and does not affect the morphology of the active layer. When blended with PM6 to make a device, how does the performance of d-Y6 compare to that of Y6?

2. To understand the formation mechanism of Y6 or d-Y6 aggregates, the singe crystal packing is more solid result compared to molecular dynamics simulation. The singe crystal of d-Y6 need to be provided.

3. The use of deuterated materials is costly and does not improve efficiency, has little application and is too costly, so the significance of this study is yet to be determined.

4. ξ in line 310 is in difference from in Table 1. Please check it.

5. The scattering lengths of hydrogen and deuterium have opposite symbols, which allows SANS to use this contrast advantage to selectively label different parts of the study target system. Whether hydrogen in PM6 and deuterium in Y6 can be detected to more deeply interpret the molecular state in the amorphous domain？

6. The author has proved that short-range aggregation behavior is unique to Y6. Whether other high-performance Y-series acceptors have similar behavior? The authors need to extend the corresponding experiment for d-L8-BO and d-BO-4Cl to support their conclusion.

7. The 13C NMR and elemental analysis of new compounds need to be provided.

Responses to comments from reviewers

We would like to thank the reviewers and the editor for their valuable time and comments, which have greatly helped to improve the quality of our paper. We have addressed the comments from each reviewer point by point and revised the manuscript accordingly. Our detailed responses are shown in blue and the corresponding revisions in both the manuscript and supplementary information are indicated with yellow highlights.

Reviewer #1:

Comments:

Reviewer #1 (Remarks to the Author):

Cai et. al. used isotrope labeling method to measure the amorphous domain size of deuterated Y6 molecules in the blend film of PM6:d-Y6 and experimentally uncovered a structure-property relationship between the short-range aggregation of Y6 molecules and the performance of OPV devices. The authors combined GISAXS and GISANS techniques to evaluate the scattering length densities of polymeric donners and acceptors, which give a large contrast to distinguish the aggregation of acceptors. Although GISANS has been widely utilized in OPV studies (refs. 28-33), the aggregation nature of Y6 in amorphous domains is significant to understanding the role of Y6, as an emerging acceptor, in the development of high-performance solar cells. Thus, I recommend this work to publish in nature communication after the response to the following comments:

Reply: We thank the reviewer for the overall positive comments.

1) All the data in this manuscript are obtained by GISAXS and GISANS. Although these two techniques are powerful to support the conclusion, would the authors additionally provide AFM phase images to observe and evaluate the phase separation of PM6: d-Y6? To do so, the crystalline and amorphous domain sizes could be measured

directly.

Reply: We thank the reviewer for this constructive comment. To complement our scattering measurements, we measured tapping-mode AFM topography images for PM6:Y6 and PM6:*d*-Y6 blend films processed under three different conditions (as-cast, CF-opt, and CB-opt, as mentioned in the main text). AFM images of PM6:Y6 blend films are similar to those of PM6:*d*-Y6 under each processing condition. The root-mean-square (RMS) roughness of blend films increases from as-cast to CF-opt, and then to CB-opt, indicating the enhanced molecular aggregation/crystallization induced by prolonged film drying times. Since topography images partially reflect phase-separated structures in blend films, we observed spherical agglomeration in CB-opt films with sizes of tens of nm, consistent with the GISAXS fitting results presented in the main text. However, we note that the short-range Y6 aggregates probed using GISANS cannot be identified from AFM images as their sizes (5-10 nm) are below the resolution of the tip we used (Tap300Al-G, Budget Sensor), which is around 10 nm.

We added the AFM topography images to **Supplementary Fig. 20**.

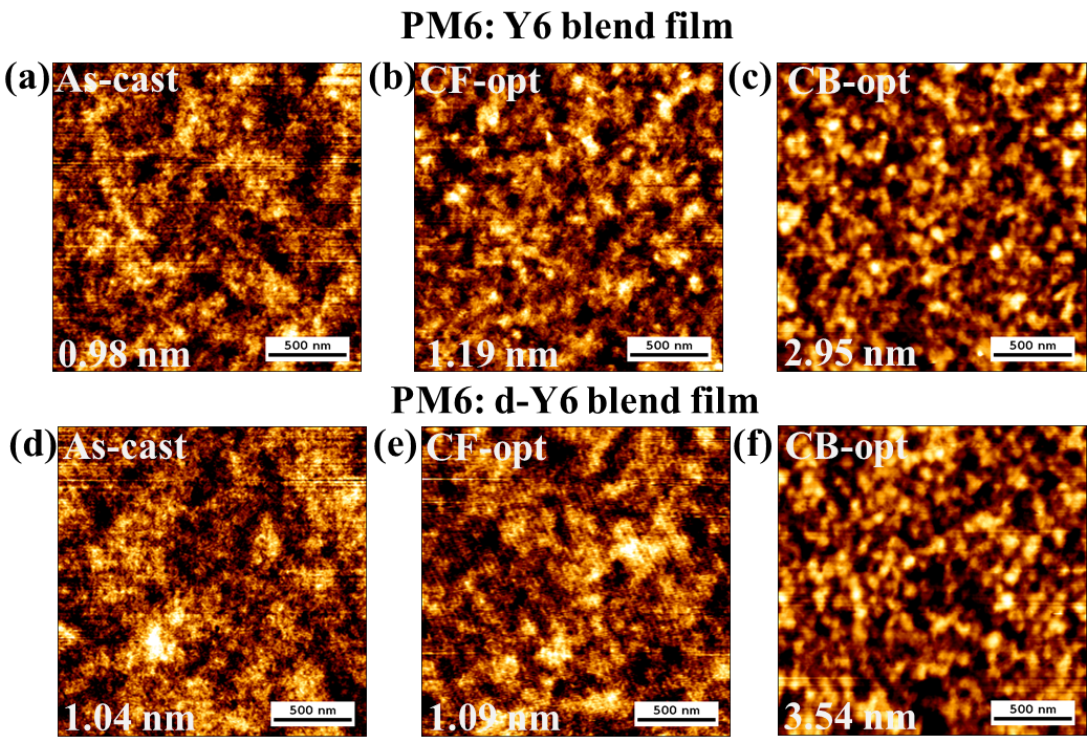

Supplementary Fig. 20 AFM topography images of PM6:Y6 (**a-c**) and PM6: *d*-Y6 (**d-**

f) blend films processed under different conditions mentioned in the main text. The root-mean-square (RMS) roughness of heights is labelled at the inset for each image.

We added the following sentences to line 293, page 16 of the main text.

Tapping-mode atomic-force microscopy (AFM) was also applied to measure the surface topography of PM6:Y6 and PM6:*d*-Y6 films processed under the three aforementioned conditions as shown in **Supplementary Fig. 20**. The spherical agglomerates with sizes of around 50 nm in CB-opt is also visible from AFM, further supporting our GISAXS fitting results. However, AFM cannot identify the short-range Y6 aggregates (5-10 nm) observed from GISANS measurements as their sizes are below the resolution limit of the AFM tip we used (around 10 nm, see **Methods**).

We added the following sentences to line 470, page 26 of the main text.

AFM measurements JPK NanoWizard NanoOptics atomic force microscope (AFM) with a Tap300Al-G tip (40 N/m) was used for topography characterization of blend films. Measurements were carried out using non-contact mode with a piezoelectric tip oscillating at a fixed frequency (300 kHz) above the sample surface. For each measurement, tip was scanned over 256 pixels across a 2 μm range at a rate of 1 Hz. A 2×2 μm image was obtained for each sample. The root-mean-square (RMS) height fluctuations were obtained using the JPKSPM Data Processing software package.

2) The authors fitted the GISAXS and GISANS intensity profile using equation 1, and provided the Information of nanomorphology in PM6: *d*-Y6 film. In line 226-227, they claim that GISAXS profile gave "the correlation length (ξ) of the amorphous intermixing phase and the size of the crystalline acceptor domain." In my opinions, both the PM6 and d-Y6 are crystalline in the blend films, so why only crystalline domain of Y6 acceptor can be evaluated by fitting the equation?

Reply: We thank the reviewer for pointing out the potential confusion. The scattering contrast of a blend film under X-ray arises from the different SLDs of constituent materials. For PM6 and Y6 with similar carbon/hydrogen compositions, this is mainly induced by their different degree of crystallinity in blend films. Based on our previous experience, NFA small molecules typically show stronger scattering of X-ray than D:A polymer donor due to their stronger degree of crystallinity [*Nat. Commun*. 12, 6226 (2021)]. Furthermore, in the blend film, it has been shown that Y6 tend to form denser and stronger crystals in blend films, substantially reducing the crystallinity of PM6 [*Adv Mater*, e2302005 (2023)]. Therefore, for the fitting of our GISAXS results, we choose the DAB model to account for the amorphous region of the PM6/*d*-Y6 mixtures and the fractal model to account for the *d*-Y6 crystalline domains.

3) Would the authors explain the reason to choose a PM6:Y6 BHJ blend as the active layers in OPV devices instead of PM6: d-Y6? Since all the information on the nanomorphology of blend films comes from PM6: d-Y6, the corresponding devices are better to be tested for data consistency, although the performance of two devices comprising PM6:Y6 and PM6: d-Y6 may be identical (as shown in Fig. S8b)

Others:

Reply: We thank the reviewer for the insightful suggestions. The reason we chose to display the data of PM6:Y6 in the main text is to emphasis that the GISANS results we obtained from PM6:*d*-Y6 are also applicable to normal non-deuterated devices. Deuteration is expensive, we have no intention to apply deuteration to improve the

device performance, which is also not feasible for mass production. We just want to employ it as a powerful labeling tool for the research of OPV morphology.

To understand the impact of deuteration on morphology, optoelectronic properties, and device performance, we have shown in **Fig. 1c**, **d**, and **Supplementary Fig. 10-12** that deuteration does not change the morphological of Y6 molecules in neat and blend films and thus does not notably impact on and optoelectronic properties and device performance. We further fabricated a new batch of PM6:Y6 and PM6:*d*-Y6 devices under three different processing conditions mentioned in the main text to compare their performances as shown in **Supplementary Fig. 17** and summarized their detailed device parameters in **Supplementary Table 3**.

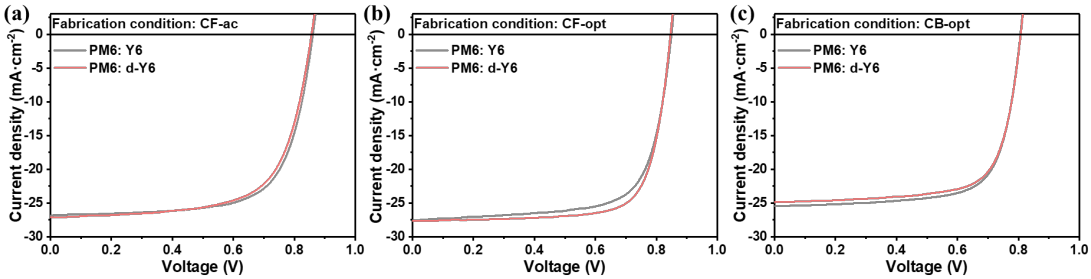

Supplementary Fig. 17 Typical J-V curves of the devices based on PM6:Y6 and PM6:*d*-Y6 under three different conditions (**a** CF-ac, **b** CF-opt, **c** CB-opt) mentioned in the main text.

Supplementary Table 3 A summary of device characteristics of PM6:Y6 and PM6:*d*-Y6 systems under three different processing conditions mentioned in the main text.

Blends	*Voc (V)* [d]	*Jsc (mA·cm^{-2})* [d]	*FF (%)* [d]	*PCE (%)* [d]
PM6: Y6 [a]	0.865 (0.861±0.003)	26.9 (26.7±0.2)	69.7 (69.0±0.5)	16.3 (15.9±0.3)
PM6: d-Y6 [a]	0.856 (0.855±0.003)	27.1 (26.7±0.3)	67.2 (66.8±0.5)	15.6 (15.2±0.2)
PM6: Y6 [b]	0.853 (0.850±0.002)	28.0 (27.7±0.5)	74.4 (74.1±0.4)	17.8 (17.4±0.3)
PM6: d-Y6 [b]	0.846 (0.843±0.002)	27.7 (27.7±0.2)	75.1 (74.7±0.3)	17.6 (17.4±0.2)
PM6: Y6 [c]	0.806 (0.798±0.006)	25.5 (24.7±0.6)	72.2 (71.5±0.5)	14.8 (14.1±0.5)
PM6: d-Y6 [c]	0.807 (0.807±0.003)	24.9 (24.6±0.5)	72.1 (72.0±0.4)	14.5 (14.3±0.2)

[a] As-cast w/o CN & TA. [b] CF-opt (w/ 0.5% CN & TA 90℃ 5min). [c] CB-opt (w/ 0.5% CN & TA 90℃ 5min).[d] Average values with their standard deviations (in parentheses) are obtained from 5 independent devices.

PM6:Y6 and PM6:*d*-Y6 show similar performances in terms of all three photovoltaic parameters under each processing condition, confirming the validity of our analysis. We added the following sentences on line 272, page 15 in the main text.

Under each processing condition, PM6:Y6 and PM6:*d*-Y6 devices show similar performance as shown in **Supplementary Fig. 17** and **Supplementary Table 3,** suggesting that the GISANS results obtained from PM6:*d*-Y6 blend films are relevant for normal non-deuterated devices as well.

We updated the device performances in Table 1 of the main text.

Table 1 A summary of fitted domain sizes and device characteristics of PM6:Y6 systems.

Samples [a]	ξ (nm)	$2R_{gc}$ (nm)	$2R_{ga}$ (nm)	V_{OC} [b] (V)	J_{SC} [b] (mA cm^{-2})	FF [b] (%)	PCE [b] (%)
CF-ac	45.6	33.1	7.8	0.865 (0.861±0.003)	26.9 (26.7±0.2)	69.7 (69.0±0.5)	16.3 (15.9±0.3)

CF-opt	49.4	29.4	10.7	0.853 (0.850±0.002)	28.0 (27.7±0.5)	74.4 (74.1±0.4)	17.8 (17.4±0.3)
CB-opt	N/A	58.1[c]	7.5	0.806 (0.798±0.006)	25.5 (24.7±0.6)	72.2 (71.5±0.5)	14.8 (14.1±0.5)

[a] D/A = 1/1.2 (w/w). [b] Average values with their standard deviations (in parentheses) are obtained from 15 independent devices. [c] The $2R_{gc}$ of the CB-opt film is obtained from the GISAXS fitting.

4) line 57, the “research” should be plural so “has” is used wrongly in grammar.

Reply: Thanks for your correction; we have already made the necessary changes.

5) line 91, the “challenghg” is a typo.

Reply: Thanks for your correction; we have already made the necessary changes.

6) line 103, “not” in the term of “it originates not from crystalline phases...” is inappropriately expressed in grammar.

Reply: Thanks for your correction; we have already made the necessary changes.

7) line 129, the “aggregation” should be singular.

Reply: Thanks for your correction; we have already made the necessary changes.

8) line 137, “Supplementary Fig. 6” should be “Supplementary Fig. 7”.

Reply: Thanks for your correction; we have already made the necessary changes.

9) line 202, the correspondence of fig. 3a and 3b to GISANS and GISAXS is an error.

Reply: Thanks for your correction; we have already made the necessary changes.

Reviewer #2:

Comments:

The main novelty of this work is that the authors deuterated the non-fullerene acceptor (NFA) Y6 to overcome the lack of neutron contrast in OPV films based on NFAs. This allowed them to study the nano-morphology of the OPV films using GISANS. This work is merely incremental, and it lacks the originality needed to be published in this journal.

In the abstract the authors say that their work uncovers "for the first time" the amorphous nanomorphology of OPV films. This is not correct – this has been addressed before either using neutron scattering or Resonant Soft X-ray Scattering (RSoXS) techniques.

Neutron scattering (SANS and Neutron reflectivity) have been previously used extensively to study fullerene-based OPVs and the authors are advised to improve their literature survey and include some important references that are missing. For example, these below among many others.

Wienhold, K.S., “Organic solar cells probed with advanced neutron scattering techniques” Applied Physics Letters, 116, 120504 (2020)

Zhang, Y. et al, "Understanding and controlling morphology evolution via DIO plasticization in PffBT4T-2OD/PC71BM devices", Scientific Reports 7, 44269 (2017)

Chen D. “P3HT/PCBM Bulk Heterojunction Organic Photovoltaics: Correlating Efficiency and Morphology”, Nano Lett. 2011, 11, 2, 561–567

Bernardo, G. et al "Impact of 1,8-diiodooctane on the morphology of organic photovoltaic (OPV) devices – A Small Angle Neutron Scattering (SANS) study", Polymer Testing 82 (2020) 106305

Reply: We appreciate the reviewer’s insightful comments and suggestions. We believe there may be a misunderstanding regarding our definition of “amorphous

nanomorphology of organic photovoltaic thin films". In our work, it refers to morphology within the **amorphous donor:acceptor intermixed domains**. Through a thorough literature search, we have ensured that this morphology has not been detected previously.

Next, we agree that neutron scattering techniques, including SANS and Neutron reflectivity, have been previously used extensively to study **fullerene-based OPVs.** In the introduction section of the original manuscript (line 76-90, page 5), we wrote:

Small-angle neutron scattering (SANS) and neutron reflectivity (NR) have been employed to investigate the nanostructure of organic solar cells based on fullerene acceptors since the dominant carbon components in fullerene derivatives provide sufficient SLD contrast relative to organic donor materials[28,29]. In a study by Dadmun *et al.*, SANS was utilized for the first time to reveal the miscibility of PCBM in P3HT, the average PCBM domain size, and the interfacial area between PCBM and the P3HT-rich phase[30]. The results of SANS experiments conducted by Nedoma et al. indicated that the phase separation between PCBM and P3HT could be controlled by device fabrication conditions[31]. In 1999, P. Müller-Buschbaum *et al.* developed grazing incidence small-angle neutron scattering (GISANS) to enhance the signal-to-noise ratio and scattering volume with the grazing incidence geometry[32]. In subsequent studies, Matthias *et al.* first applied GISANS in OPV studies and investigated the phase separation and molecular intermixing in the P3HT/$PC_{61}BM$ bulk heterojunction[33]. In 2018, W. Wang *et al.* used time-of-flight (TOF)-GISANS in the P3HT:$PC_{61}BM$ bulk heterojunction thin film and quantitatively determined the molecular miscibility between P3HT and $PC_{61}BM$ as well as the depth-dependent morphology changes induced by additives[28].

We also thank the reviewer for reminding us of more relevant literature. Particularly,

the paper [*Chem. Phys.* 427, 142-146 (2013).] introduced a new quasi-elastic neutron scattering (QENS) to monitor the motions of the polymer side-chains of P3HT which were slowed down upon addition and further crystallization of the PCBM molecules. We have added all references mentioned by the reviewer to the following paragraph on page 5 of the revised main text.

Small-angle neutron scattering (SANS), neutron reflectivity (NR) and quasi-elastic neutron scattering (QENS) have been employed to investigate the nanostructure, dynamic fluctuations of OPV active layers composed of fullerene acceptors since the dominant carbon components in fullerene derivatives provide sufficient SLD contrast relative to organic donor materials[28,29]. In the study by Dadmun *et al.*, SANS was utilized for the first time to reveal the miscibility of PCBM in P3HT, the average PCBM domain size, and the interfacial area between PCBM and the P3HT-rich phases[30]. The results of SANS experiments conducted by Nedoma et al. indicated that the phase separation between PCBM and P3HT could be controlled by device fabrication conditions[31]. More following research also demonstrated the nanomorphology of fullerene based organic solar cells by SANS[32-34]. In terms of dynamic information, quasi-elastic neutron scattering (QENS) was utilized to monitor the motions of the side-chains of P3HT polymers which were slowed down upon addition and further crystallization of the PCBM molecules[35,36]. In 1999, P. Müller-Buschbaum *et al.* developed grazing incidence small-angle neutron scattering (GISANS) to enhance the signal-to-noise ratio and scattering volume with the grazing incidence geometry[37]. Matthias *et al.* first applied GISANS in OPV studies and investigated the phase separation and molecular intermixing in the P3HT/$PC_{61}BM$ bulk heterojunction[38]. Subsequently, this technique was applied by Guo *et al.* to study the impact of alcohol post treatment on inner phase structure of PTB7:$PC_{71}BM$ blend films[39].

In summary, all these references are focused on using transmission-mode SANS or

GISANS to probe the morphology of fullerene-based blend films, taking advantage of the much stronger scattering contrast between fullerene molecules and polymer donors under neutron beam. The same methodology cannot be directly transferred to polymer:non-fullerene acceptor (NFA) blend films where donor and acceptor molecules have similar carbon: hydrogen ratios and thus similar SLDs under both X-ray and neutron. This challenge motivates us to combine targeted deuteration and GISANS to further probe morphology in these NFA-based blend systems. Therefore, the references mentioned by the reviewer do not undermine the originality of our work but rather highlighting the innovation in our approach.

We added the following works to our reference list.

32 Bernardo, G. *et al.* Impact of 1,8-diiodooctane on the morphology of organic photovoltaic (opv) devices – a small angle neutron scattering (sans) study. *Polymer Testing* **82** (2020).

33 Chen, D., Nakahara, A., Wei, D., Nordlund, D. & Russell, T. P. P3ht/pcbm bulk heterojunction organic photovoltaics: Correlating efficiency and morphology. *Nano Lett* **11,** 561-567 (2011).

34 Zhang, Y. *et al.* Understanding and controlling morphology evolution via dio plasticization in pffbt4t-2od/pc(71)bm devices. *Sci Rep* **7,** 44269 (2017).

35 Paternó, G., Cacialli, F. & García-Sakai, V. Structural and dynamical characterization of p3ht/pcbm blends. *Chem. Phys.* **427,** 142-146 (2013).

36 Wienhold, K. S., Jiang, X. & Müller-Buschbaum, P. Organic solar cells probed with advanced neutron scattering techniques. *Appl. Phys. Lett.* **116** (2020).

39 Guo, S., Cao, B., Wang, W., Moulin, J.-F. & Müller-Buschbaum, P. Effect of alcohol treatment on the performance of ptb7:Pc71bm bulk heterojunction solar cells. *ACS Appl. Mater. Interfaces* **7,** 4641-4649 (2015).

Reviewer #3:

Comments:

Reviewer #3 (Remarks to the Author):

The authors used a combination of neutron scattering - in terms of GISANS technique

- and deuteration to probe the nanomorphology of the PM6:d-Y6 blend film. The deuteration was selectively done for the NFA Y6 (d-Y6). The measurements were underpinned by MD calculations. The study highlighted a specific short-range aggregation of Y6 - as an intrinsic feature of this NFA, that was concluded to be a key contributor to the high photovoltaic performance of most Y6-containing organic bulk heterojunction systems. Indeed, the authors studied other polymers than PM6, and have supported the neutron data by measurements using different x-ray and light-based techniques.

The manuscript is dense, organized and well written. The topic, techniques and findings warrant publication in Nature Communications after considering the following comment.

The only concern readers, who might be interested in applying neutron scattering and associated deuteration in their research on OPVs, would be to have some more targeted references on the application of neutron scattering and deuteration to study morphology and local properties, including dynamics, beyond GISANS by including other neutron-based techniques. In this context, the authors are invited to enrich the introduction and the reference list by considering recent works on binary and ternary blend, either with acceptors being fullerenes (PCBM, etc) or NFAs (O-IDTBR, etc).

Reply: We really appreciate the reviewer's positive comments and insightful suggestions. Following the reviewer's suggestion, we have enriched introduction and the reference list by including more important works on ternary OPVs incorporating either fullerene-based acceptors [*J. Mater. Chem. A* 7, 20713-20722 (2019)] or NFAs like IDTBR [*Nat. Mater.* 16, 363-369 (2017).] and Y6 [*Dyes Pigm.* 181, 108613 (2020)] as the third component. We pointed out that despite the ternary (and quaternary) has improved the efficiency and stability of OPVs, the exact microscopic origin remains under debate [*Nat. Rev. Mater.* 8, 456-471 (2023). & *Nat. Energy* 8, 978-988 (2023)]. This can be largely attributed to the similar chemical structures between donor and

297 acceptor materials (in case of NFAs) or the fact that the amount of dopant added is small
298 compared to the host materials (in case of fullerenes) that renders morphology
299 characterization challenging. This dilemma could potentially be resolved by combining
300 deuteration labelling and GISANS, which will the focus of our future work.
301
302 We added the following sentences to line 105 of page 6.
303
304 The same issue also hinders the full characterization of ternary (and quaternary) blend
305 films because the dopants used typically have similar chemical structures with host
306 materials or the amount of dopants added is small. Therefore, although ternary
307 strategies incorporating both fullerene[40] and NFAs (e.g. IDTBR[41] and Y6[42]) have
308 proved effective in improving the efficiency and stability of OPVs, the exact
309 microscopic origin remains controversial[43,44].
310
311 In addition to SANS and GISANS, we also added a brief introduction on quasi-elastic
312 neutron scattering (QENS) on line 91 of page 5.
313
314 In terms of dynamic information, quasi-elastic neutron scattering (QENS) was utilized
315 to monitor the motions of the polymer side-chains of P3HT which were slowed down
316 upon addition and further crystallization of the PCBM molecules[35,36].
317
318
319 We have also reviewed a few more examples of previous studies combining deuteration
320 and neutron scattering in other fields beyond organic photovoltaics on line 111 of page
321 6.
322
323 This technique has been previously applied to study e.g., the structure of conducting
324 polymers[45] and biological macromolecules[46], yet it has not been applied to probe the

morphology of OPV active layers.

The following references were added to the main text.

35 Paternó, G., Cacialli, F. & García-Sakai, V. Structural and dynamical characterization of p3ht/pcbm blends. *Chem. Phys.* **427,** 142-146 (2013).

36 Wienhold, K. S., Jiang, X. & Müller-Buschbaum, P. Organic solar cells probed with advanced neutron scattering techniques. *Appl. Phys. Lett.* **116** (2020).

40 Pan, M.-A. *et al.* 16.7%-efficiency ternary blended organic photovoltaic cells with pcbm as the acceptor additive to increase the open-circuit voltage and phase purity. *J. Mater. Chem. A* **7,** 20713-20722 (2019).

41 Baran, D. *et al.* Reducing the efficiency–stability–cost gap of organic photovoltaics with highly efficient and stable small molecule acceptor ternary solar cells. *Nat. Mater.* **16,** 363-369 (2017).

42 Jiang, B.-H. *et al.* The role of y6 as the third component in fullerene-free ternary organic photovoltaics. *Dyes Pigm.* **181,** 108613 (2020).

43 Günther, M. *et al.* Models and mechanisms of ternary organic solar cells. *Nature Reviews Materials* **8,** 456-471 (2023).

44 Wang, Y. *et al.* Origins of the open-circuit voltage in ternary organic solar cells and design rules for minimized voltage losses. *Nature Energy* **8,** 978-988 (2023).

45 Shao, M. *et al.* The isotopic effects of deuteration on optoelectronic properties of conducting polymers. *Nat Commun* **5,** 3180 (2014).

46 Jeffries, C. M. *et al.* Preparing monodisperse macromolecular samples for successful biological small-angle x-ray and neutron-scattering experiments. *Nat Protoc* **11,** 2122-2153 (2016).

Reviewer #4:

Comments:

Reviewer #4 (Remarks to the Author):

Deuteration-enhanced neutron is cleverly applied to GISANS test, and the unique short-range aggregation behavior of Y6 in the D/A blending region is effectively detected, which also confirms the experimental results of other research groups. Prof Lu and co-workers provide a novel method for detecting the aggregate state of non-crystalline domain in active layer of OSCs. However, SANS is already a conventional and mature characterization technique, and deuterated materials have also been applied to SANS.

In addition, the PM6:Y6 device in the paper is a very conventional, although the authors claim that directionally deuterated SANS technology offers opportunities for complex active layer systems and intermolecular interaction mechanisms. The innovation of this article is insufficient. The authors did not validate the proposed large short-range aggregation of acceptors in the D/A blend region as a key to recent high-performance organic solar cells and provide insights for improving the efficiency or stability of organic solar cells, so it is not recommended for publication in Nature Communication.

Reply: We appreciate the thoughtful comments provided by the reviewer and have carefully addressed them point-by-point as detailed in the following response. In response to the observation that SANS and deuteration have been previously applied together, we wish to highlight the unique contribution of our work. While this combination has been utilized in other fields, for instance, biology systems, our work represents the first application to investigate the amorphous nanomorphology in organic photovoltaic thin films. In addition, the reason we chose to use the conventional system of PM6:Y6 to demonstrate this methodology is because we want to highlight its generality, while recent advancements on OPV performance often utilize Y-series acceptors. Following the reviewer's suggestion, in the revised manuscript, we further deuterate another Y-series molecule-Y7 to demonstrate the generality of our results.

2. Prof. Ye has demonstrated that deuterated solvents can improve the performance of organic solar cells (Aggregate 2023, 4, e289). d-Y6 shows similar photoelectric properties to Y6 and does not affect the morphology of the active layer. When blended with PM6 to make a device, how does the performance of d-Y6 compare to that of Y6?

Reply: We thank the reviewer for reminding us of this important work. In Prof. Ye's work, the deuterium substitution is on **solvent molecules**, not **acceptors**. The deuterated solvent reduces their molar volume and polarizability by decreasing the

length and dipole moment of C-H bonds, resulting in suppressed solubility parameter (δ) of active layer materials in deuterated solvents, and therefore increase the crystallinity of the casted film. We did not observe similar device performance improvement with the deuteration of Y6. Prof. Ye and co-workers recently

In **Supplementary Fig. 11** and **12b**, we have shown that PM6:Y6 and PM6:*d*-Y6 blend films have similar crystal structures and photovoltaic performances. To further stress this point, we also compared PM6:Y6 and PM6:*d*-Y6 devices fabricated under three different conditions (as-cast, CF-opt, and CB-opt). Under each condition, the PM6:*d*-Y6 device shows similar performance in terms of all three photovoltaic parameters (*FF*, J_{sc}, and V_{oc}) with the corresponding PM6:Y6 device. This confirms that deuteration of Y6 has negligible impact on their morphological and optoelectronic properties in both neat and blend films. We added the J-V curves to **Supplementary Fig. 17** and detailed device characteristics to **Supplementary Table 3.**

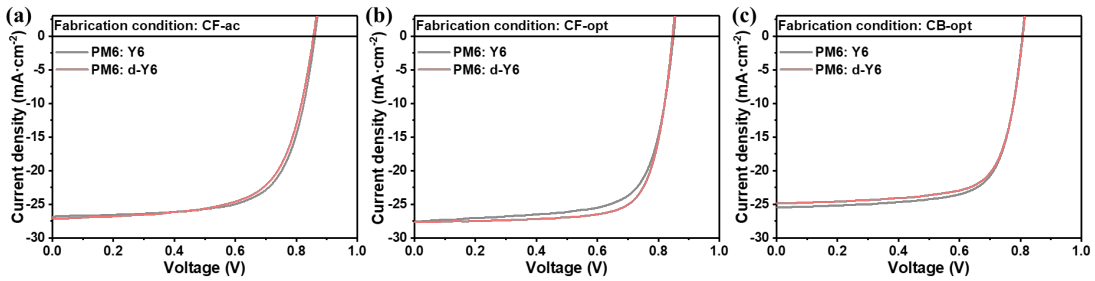

Supplementary Fig. 17 Typical J-V curves of the devices based on PM6:Y6 and PM6:*d*-Y6 under three different conditions (**a** CF-ac, **b** CF-opt, **c** CB-opt) mentioned in the main text.

Supplementary Table 3 A summary of device characteristics of PM6:Y6 and PM6:*d*-Y6 systems under three different processing conditions mentioned in the main text.

Blends	*Voc (V)* [d]	*Jsc (mA·cm^{-2})* [d]	*FF (%)* [d]	*PCE (%)* [d]
PM6: Y6 [a]	0.865 (0.861±0.003)	26.9 (26.7±0.2)	69.7 (69.0±0.5)	16.3 (15.9±0.3)
PM6: d-Y6 [a]	0.856 (0.855±0.003)	27.1 (26.7±0.3)	67.2 (66.8±0.5)	15.6 (15.2±0.2)
PM6: Y6 [b]	0.853 (0.850±0.002)	28.0 (27.7±0.5)	74.4 (74.1±0.4)	17.8 (17.4±0.3)
PM6: d-Y6 [b]	0.846 (0.843±0.002)	27.7 (27.7±0.2)	75.1 (74.7±0.3)	17.6 (17.4±0.2)
PM6: Y6 [c]	0.806 (0.798±0.006)	25.5 (24.7±0.6)	72.2 (71.5±0.5)	14.8 (14.1±0.5)
PM6: d-Y6 [c]	0.807 (0.807±0.003)	24.9 (24.6±0.5)	72.1 (72.0±0.4)	14.5 (14.3±0.2)

[a] As-cast w/o CN & TA. [b] CF-opt (w/ 0.5% CN & TA 90℃ 5min). [c] CB-opt (w/ 0.5% CN & TA 90℃ 5min).[d] Average values with their standard deviations (in parentheses) are obtained from 5 independent devices.

We also added the following sentences to line 272, page 15 of the main text.

Under each processing condition, PM6:Y6 and PM6:*d*-Y6 devices show similar performance as shown in **Supplementary Fig. 17** and **Supplementary Table 3,** suggesting that the GISANS results obtained from PM6:*d*-Y6 blend films are relevant for normal non-deuterated devices as well.

2. To understand the formation mechanism of Y6 or d-Y6 aggregates, the singe crystal packing is more solid result compared to molecular dynamics simulation. The single crystal of d-Y6 need to be provided.

Reply: Thanks a lot for the suggestion. Single-crystal analysis is a powerful tool to capture crystalline packing motifs of conjugated molecules in their thermodynamically stable states. However, this work is focusing on the **amorphous** morphology but not the crystalline packing of Y6. Furthermore, it cannot predict the formation of short-range Y6 aggregates within the **blend** film with polymer donors cast by spin coating. Therefore, we believe the single crystal analysis of d-Y6 is not necessary here and MD simulation is a more valid method to complement our experimental results to

understand the formation mechanism of short-range Y6 aggregates in thin films formed through non-equilibrium kinect process.

3. The use of deuterated materials is costly and does not improve efficiency, has little application and is too costly, so the significance of this study is yet to be determined.

Reply: We thank the reviewer for raising this important concern. Yes, the deuteration of conjugated small molecules or even polymers is costly and it does not notably affect the performance of OPV devices as we have shown in the main text. We emphasis that our goal is to apply deuteration substitution as an effective labelling technique to complement GISANS measurements so that we could reveal the previously hidden short-range structure and establish robust processing-structure-performance relationships for OPVs. Therefore, we only need to synthesis a relatively small amount of deuterated materials (e.g. several tens of mg) to help us with morphology characterizations so the cost is affordable.

4. ξ in line 310 is in difference from in Table 1. Please check it.

Reply: Thanks for your correction; we have already made the necessary changes.

5. The scattering lengths of hydrogen and deuterium have opposite symbols, which allows SANS to use this contrast advantage to selectively label different parts of the study target system. Whether hydrogen in PM6 and deuterium in Y6 can be detected to more deeply interpret the molecular state in the amorphous domain?

Reply: We thank the reviewer for this inspiring suggestion. So far, we are making use of the enhanced contrast to probe the statistical averaged domain sizes of the crystalline and amorphous Y6. If we want to obtain the molecular state in the amorphous domain, we may need to design more delicate deuteration schemes on different functional groups for PM6 and Y6 and compare the scattering difference of different combinations to extract the detailed molecular state, which is way beyond the scope of this work.

6. The author has proved that short-range aggregation behavior is unique to Y6.

Whether other high-performance Y-series acceptors have similar behavior? The authors need to extend the corresponding experiment for d-L8-BO and d-BO-4Cl to support their conclusion.

Reply: We thank the reviewer for the valuable suggestions. To prove the generality of our findings for other Y-series NFAs, in the revised manuscript, we have synthesized a new Y-series NFA - *d*-Y7, which shares the same backbone with Y6 but with chlorinated end groups [*Nat. Commun.* 10, 1-8 (2019).]. The GISANS results confirmed that *d*-Y7 shows a higher SLD of 5.37×10^{-6} Å^{-2} compared to Y7 (1.77×10^{-6} Å^{-2}). Encouragingly, the scattering feature associated with short-range aggregates was also observed in the blend film of PM6:*d*-Y7 with characteristic length of around 5.4 nm. Considering the similar molecular structures of Y6 and Y7, we anticipate that the prerequisite for forming short-range aggregates is the ability to maintain high backbone planarity. It has been shown previously that the beta side chains attached to the outer core group of Y6, regardless of their chain lengths and shapes, are crucial to suppress dihedral angle between core and end groups [*Energy Environ. Sci.* 13, 2422-2430 (2020). & *Nat. Rev. Mater.* 8, 839-852 (2023).]. Therefore, our conclusion should be general for most Y-series NFAs with side chains attached to this position.

We added the results of ^{1}H and ^{13}C NMR spectroscopy to the Supporting Information.

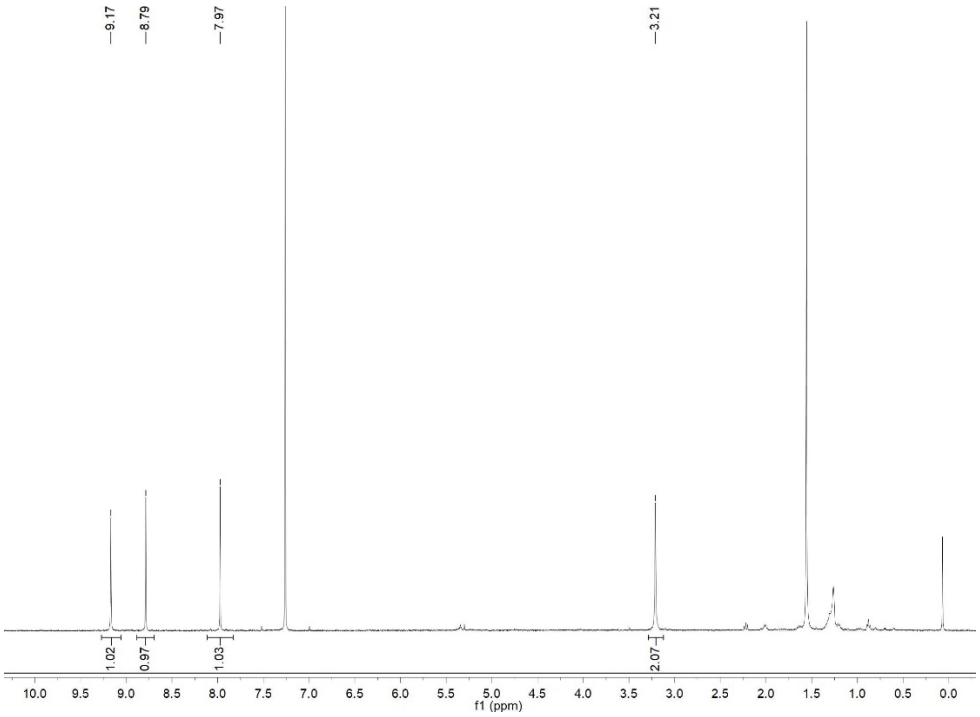

Supplementary Fig. 5 ^{1}H NMR spectrum of *d*-Y7.

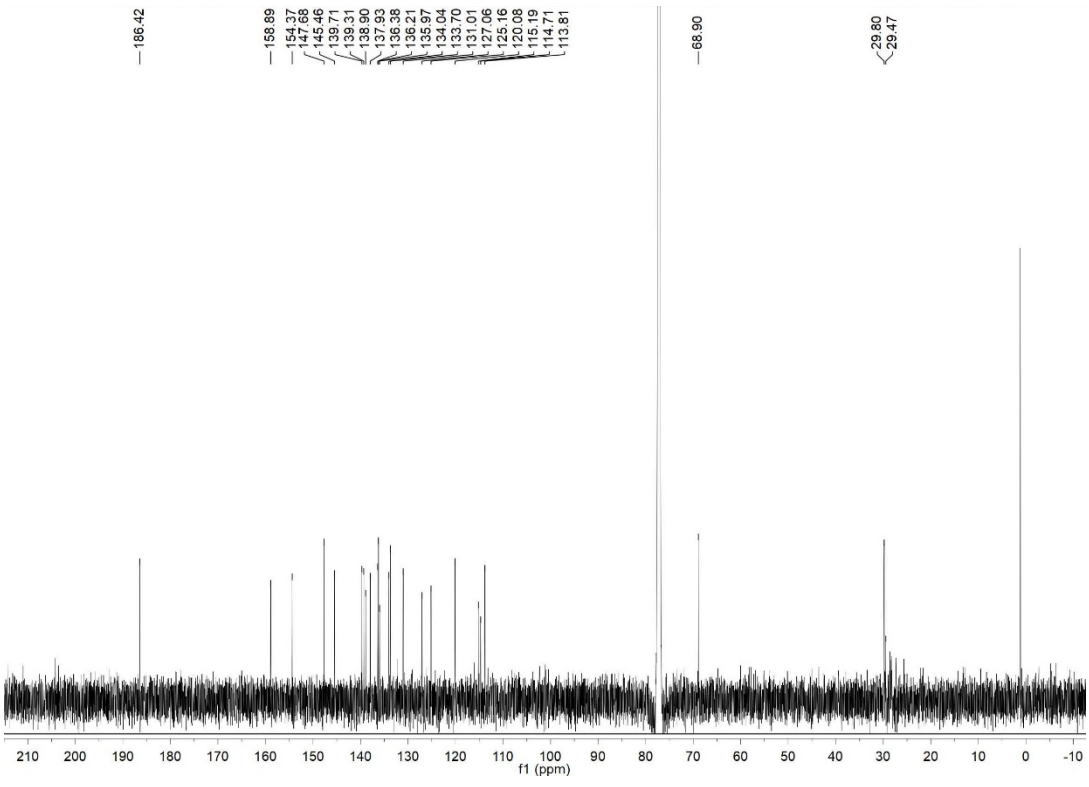

Supplementary Fig. 6 ^{13}C NMR spectrum of *d*-Y7.

***d*-Y7** The material was synthesized following the same route as *d*-Y6. ^{1}H NMR (400

MHz, Chloroform-*d*) δ 9.17 (s, 1H), 8.79 (s, 1H), 7.97 (s, 1H), 3.21 (s, 2H) ppm; ^{13}C NMR (151 MHz, Chloroform-*d*) δ 186.42, 158.89, 154.37, 147.68, 145.46, 139.71, 139.31, 138.90, 137.93, 136.38, 136.21, 135.97, 134.04, 133.70, 131.01, 127.06, 125.16, 120.08, 115.19, 114.71, 113.81, 68.90, 29.80, 29.47 ppm.

The GISANS data of PM6:*d*-Y7 was added to **Supplementary Fig. 23**.

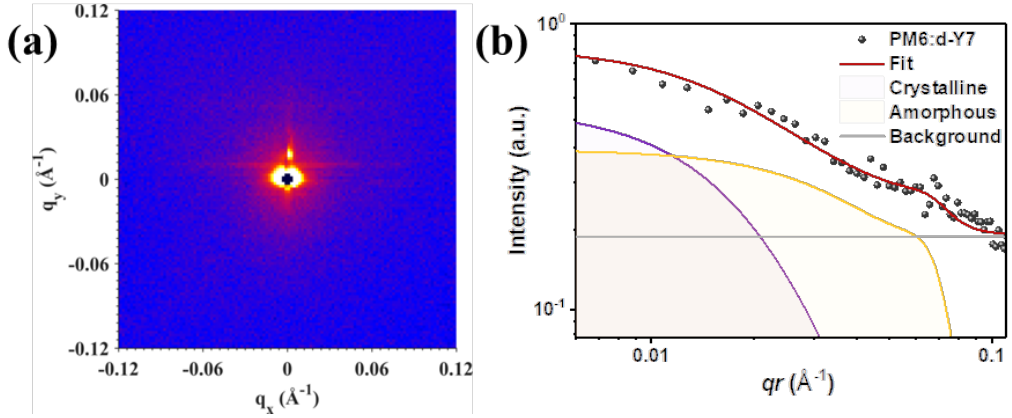

Supplementary Fig. 23 2D TOF-GISANS patterns of **a** PM6:Y7 and **b** PM6:*d*-Y7 with their horizontal linecuts (dots) with best fits (solid line) shown in **c** and **d**, respectively.

We updated domain sizes in Supplementary Table 5.

Supplementary Table 5 Morphology parameters fitted from the GISANS intensity profiles ($2R_{gc}$ is the crystallized acceptor domain size, $2R_{ga}$ is the amorphous acceptor domain size in the intermixing phase.)

Active layer	$2R_{gc}$ (nm)	$2R_{ga}$ (nm)
PM6:*d*-Y7	13.8	5.4
PM6:*d*-IDIC	22	N/A
P3HT:*d*-Y6	33.7	7.5

PTB7-Th:*d*-Y6	31.7	6.7
J71:*d*-Y6	28.7	6.7

We modified the following sentences on line 124, page 6 of the main text.

Similar aggregates were observed in the blend films of *d*-Y6 with other polymer donors as well as in the blend film of PM6 with deuterated Y7 (*d*-Y7), a chlorinated Y6 derivative[47], yet no such scattering feature was observed in the film of PM6 blended with another deuterated NFA – IDIC[48].

We modified the following sentences on line 355, page 20 of the main text.

To find out whether this short-range aggregation behavior is unique to Y-series NFAs, we performed deuteration substitution on Y7, a chlorinated Y6 derivative[47], and IDIC, another high-performance NFA modified from ITIC[48]. The synthesis of *d*-Y7 follows the same route as *d*-Y6 while the synthesis route of *d*-IDIC can be found in **Supplementary Fig. 1d**. The corresponding ^{1}H and ^{13}CNMR spectra are shown in **Supplementary Fig. 5-8**, while the mass spectroscopy and elemental analysis for *d*-IDIC can be found in **Supplementary Fig. 9** and notes of Supporting Information, respectively. Upon deuteration, the neutron SLDs increase from 1.77×10^{-6} to 5.37×10^{-6} Å^{-2} and 1.85×10^{-6} to 1.09×10^{-5} Å^{-2} for Y7 and IDIC, respectively. However, the scattering feature related to short-range aggregates was only detected in the blend film of PM6:*d*-Y7 but not in PM6:*d*-IDIC, as shown in **Supplementary Fig. 23, 24** and **Supplementary Table 5**.

We added the following sentences to line 393, page 23 of the main text.

Since this unique feature has been observed in blend films of both Y6 and Y7, it likely

arises from their excellent backbone planarity compared to ITIC-based NFAs. It has been shown that the beta side chains attached to the outer core groups of Y6 molecules, regardless of their chain lengths and shapes, can induce steric hindrance effects to suppress dihedral angles between core and end groups[61,62]. Therefore, we anticipate that our conclusion should be generally applicable to Y-series NFAs with side chains attached to the same position.

We added the following references to the main text.

61 Wu, J. *et al.* Exceptionally low charge trapping enables highly efficient organic bulk heterojunction solar cells. *Energy & Environmental Science* **13,** 2422-2430 (2020).

62 Luke, J., Yang, E. J., Labanti, C., Park, S. Y. & Kim, J.-S. Key molecular perspectives for high stability in organic photovoltaics. *Nature Reviews Materials* **8,** 839-852 (2023).

We added the following co-authors who synthesized *d*-Y7 to the author list.

Guilong Cai[1,3,10], Yuhao Li[1,2,10]*, Yuang Fu[1,10], Hua Yang[2], Le Mei[4], Zhaoyang Nie[5], Tengfei Li[6], Heng Liu[1], Yubin Ke[2], Xun-Li Wang[7,8], Jean-Luc Brédas[9], Man-Chung Tang[5], Xiankai Chen[4], Xiaowei Zhan[6,]* and Xinhui Lu[1,]*

[5] Institute of Materials Research, Tsinghua Shenzhen International Graduate School, Tsinghua University, 518055 Shenzhen, China.

We included their contributions to this manuscript on line 557, page 30 of the main text.

Z.N., M.-C.T. synthesized *d*-Y7.

7 . The 13C NMR and elemental analysis of new compounds need to be provided.

Reply: We thanks the reviewer for this important suggestion. We have added the ^{13}C NMR spectra and elemental analysis results of *d*-Y6 and *d*-IDIC to the Supporting Information.

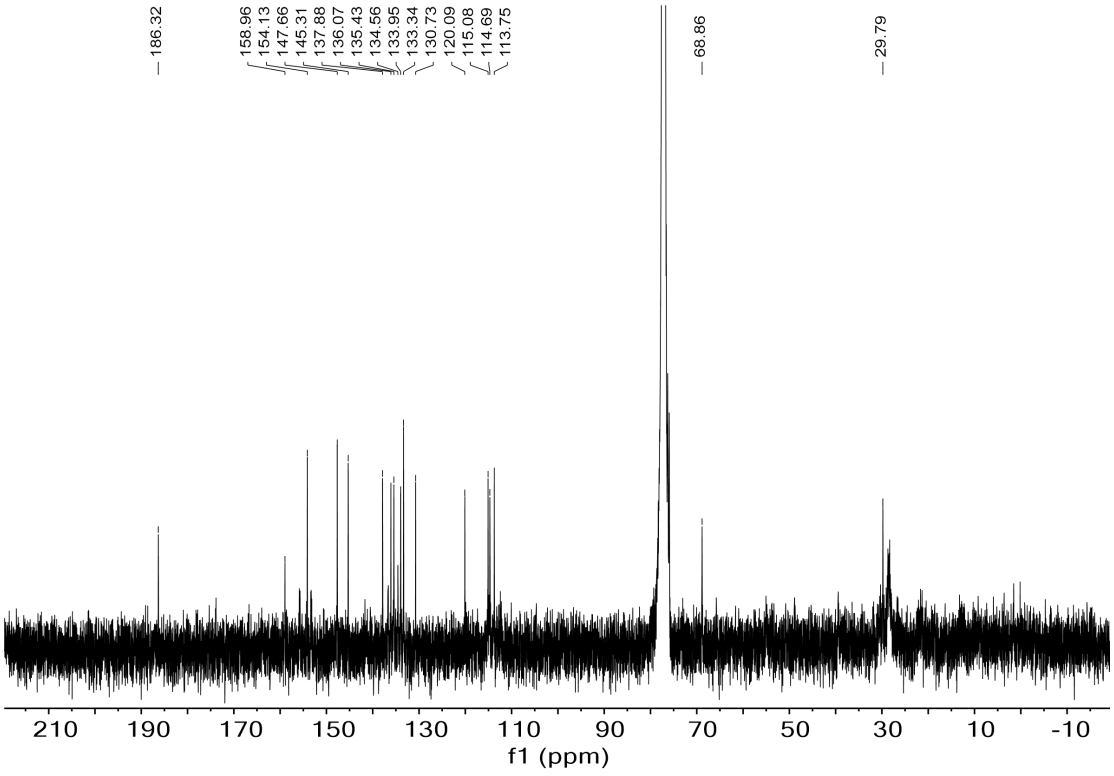

Supplementary Fig. 3 ^{13}C NMR spectrum of *d*-Y6.

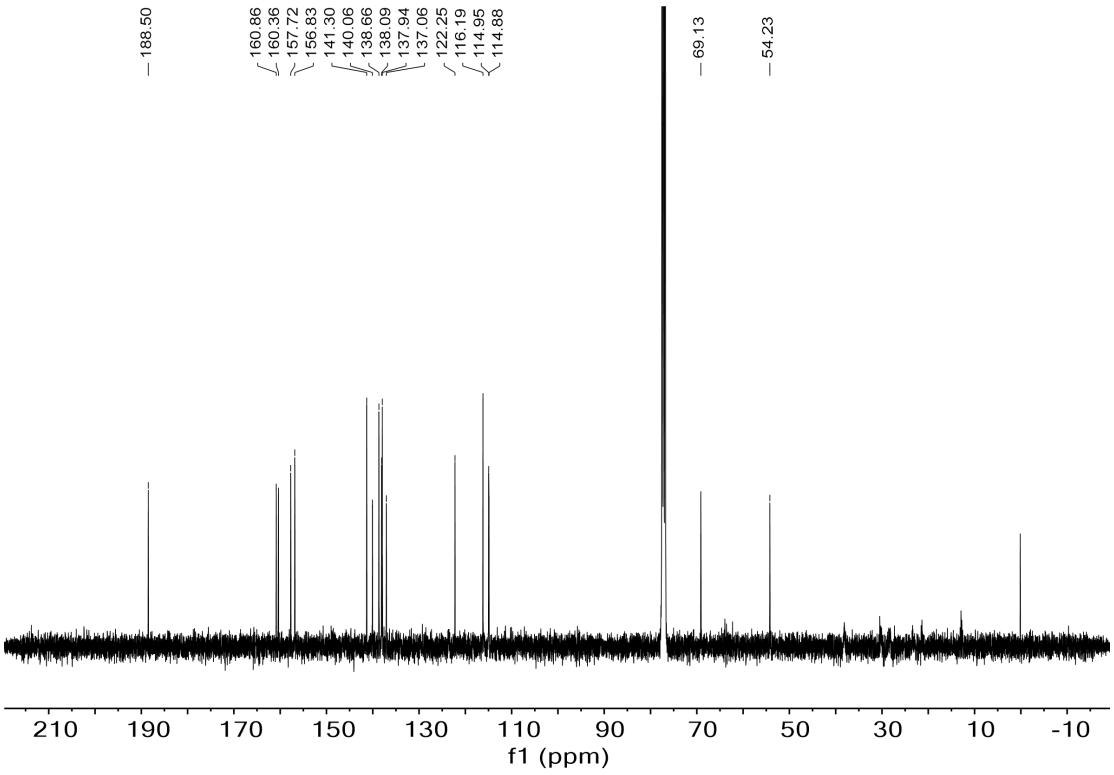

Supplementary Fig. 8 ^{13}C NMR spectrum of *d*-IDIC.

***d*-Y6.** To a three-necked round bottom flask were added Compound 5 (220 mg, 0.2 mmol), *d*-2FIC (140 mg, 0.6 mmol), pyridine (0.15 mL) and chloroform (25 mL). The mixture was deoxygenated with nitrogen for 20 min and then stirred at reflux for 12 h. After cooling to room temperature, the mixture was poured into methanol (200 mL) and filtered. The residue was purified by column chromatography on silica gel using a mixture solvent as eluent (petroleum ether/dichloromethane, v/v = 1/1) to give a blue solid (255 mg, 83%). ^{1}H NMR (400 MHz, Chloroform-*d*) δ 9.2 (s, 2H), 3.2 (s, 4H). ^{13}C NMR (100 MHz, Chloroform-*d*) δ 186.3, 159.0, 154.1, 147.7, 145.3, 137.9, 136.1, 135.4, 134.6, 134.0, 133.3, 130.7, 120.1, 115.1, 114.7, 113.7, 68.9, 29.8. HRMS (MALDI) calculated for $C_{82}H_6D_{80}F_4N_8O_2S_5$: 1531.0429; found: 1531.0424 (M^+). Elemental analysis calculated for $C_{82}H_7D_{80}F_4N_8O_2S_5$: C, 64.23; N, 7.31. Found: C,

64.12; N, 7.13.

***d*-IDIC.** To a three-necked round bottom flask were added Compound S12 (142 mg, 0.2 mmol), *d*-IC (120 mg, 0.6 mmol), pyridine (0.15 mL) and chloroform (25 mL). The mixture was deoxygenated with nitrogen for 20 min and then stirred at reflux for 12 h. After cooling to room temperature, the mixture was poured into methanol (200 mL) and filtered. The residue was purified by column chromatography on silica gel using a mixture solvent as eluent (petroleum ether/dichloromethane, v/v = 1/1) to give a blue solid (173 mg, 81%). ^{1}H NMR (400 MHz, Chloroform-*d*) δ 9.0 (s, 2H), 7.7 (s, 2H), 7.6 (s, 2H). ^{13}C NMR (100 MHz, Chloroform-*d*) δ 188.5, 160.9, 160.4, 157.7, 156.8, 141.3, 140.1, 138.7, 138.1, 137.9, 137.1, 122.2, 116.2, 115.0, 114.9, 69.1, 54.2. HRMS (MALDI) calculated for $C_{66}H_6D_{60}N_4O_2S_2$: 1070.8388; found: 1070.8384 (M^+). Elemental analysis calculated for $C_{66}H_6D_{60}N_4O_2S_2$: C, 73.96; N, 5.23. Found: C, 73.56; N, 5.07.

We modified the following sentence on line 145 of page 9.

The new compounds were fully characterized using ^{1}H and ^{13}C nuclear magnetic resonance (NMR) spectroscopy, mass spectrometry, and elemental analysis as shown in **Fig. 1b**, **Supplementary Fig. 2-4**, and note in Supporting Information, respectively.

REVIEWERS' COMMENTS

Reviewer #1 (Remarks to the Author):

The authors have been fully addressed my concerns. The manuscript could be published as this version.

Reviewer #2 (Remarks to the Author):

The authors have carefully addressed all the reviewer comments and have substantially improved their literature survey.

In the discussion of their results the authors were now able to convince me about the originality of their work. In particular, is original the combination of NFA deuteration and GISANS to unravel the short-range aggregation of Y6 molecules embedded within the amorphous intermixing phase of polymer/Y6. As far as I know, this type of morphology has not been previously reported in BHJ OPVs. This work highlights the unique morphological advantage of Y6 and the important role of short-range aggregation in OPV performance.

I recommend this work to publish in Nature Communications in its current form.

Reviewer #3 (Remarks to the Author):

The authors addressed comments and amended the manuscript accordingly. Therefore I recommend its publication.

Reviewer #4 (Remarks to the Author):

In the revised manuscript, although part of the problems was addressed, some of key issues remain unaddressed clearly.

1) The use of deuterated materials is costly and does not improve efficiency, has little application and is too costly, please give a cost analysis for the synthesis of corresponding deuterated materials in comparison with the conventional materials.

2) d-L8-BO and d-BO-4Cl are more popular and more efficient Y-series acceptors and they showed different amount and type of deuterated atoms, the corresponding experiment for d-L8-BO and d-BO-4Cl will be more support their conclusion.

3) Carbon-fluorine coupling (in 13C) for d-Y6 and d-L8-BO should be included in NMR data.

Responses to comments from reviewers

We would like to thank the reviewers and the editor for their valuable time and comments, which have greatly helped to improve the quality of our paper. We have addressed the comments from each reviewer point by point and revised the manuscript accordingly. Our detailed responses are shown in blue and the corresponding revisions in both the manuscript and supplementary information are indicated with yellow highlights.

Reviewer #1:

Comments:

The authors have been fully addressed my concerns. The manuscript could be published as this version.

Reply: We thank the reviewer for the positive comments.

Reviewer #2:

Comments:

The authors have carefully addressed all the reviewer comments and have substantially improved their literature survey.

In the discussion of their results the authors were now able to convince me about the originality of their work. In particular, is original the combination of NFA deuteration and GISANS to unravel the short-range aggregation of Y6 molecules embedded within the amorphous intermixing phase of polymer/Y6. As far as I know, this type of morphology has not been previously reported in BHJ OPVs. This work highlights the unique morphological advantage of Y6 and the important role of short-range aggregation in OPV performance.

I recommend this work to publish in Nature Communications in its current form.

Reply: We appreciate the reviewer's insightful comments and suggestions.

Reviewer #3:

Comments:

The authors addressed comments and amended the manuscript accordingly. Therefore I recommend its publication.

Reply: We really appreciate the reviewer's positive comments and insightful suggestions.

Reviewer #4:

Comments:

In the revised manuscript, although part of the problems was addressed, some of key issues remain unaddressed clearly.

1) The use of deuterated materials is costly and does not improve efficiency, has little application and is too costly, please give a cost analysis for the synthesis of corresponding deuterated materials in comparison with the conventional materials.

Reply: We agree with the reviewer that the deuteration of OPV active layer materials is costly. However, we meant to apply it as a labelling technique to probe the morphology of novel organic blend films so the material consumption per project would be low. We quote from the work by Li et al. [*Synth. Met.* 281, 116904 (2021).] that the synthesis cost of Y6 molecules is 1000 USD/g. Since the prices of deuterated components are on average 2 to 3 times higher than the corresponding non-deuterated ones, we estimate that the cost of *d*-Y6 molecules would be around 2500 USD/g. In this project, we have only used around 50 mg of *d*-Y6, corresponding to a total cost of $125. Therefore, we believe that targeted deuteration is cost-worthy and could be applied to study other novel organic optoelectronic materials in the future.

2) d-L8-BO and d-BO-4Cl are more popular and more efficient Y-series acceptors and they showed different amount and type of deuterated atoms, the corresponding

experiment for d-L8-BO and d-BO-4Cl will be more support their conclusion.

Reply: We thank the reviewer for raising this important concern. We chose to deuterate Y7, because it has similar chemical structure to Y6, as an easy and fast showcase for the generality of our work. In the coming work, we indeed to plan to extend our study to more high-performance Y-series molecules such as L8-BO and BO-4Cl to establish structure-performance relationships.

3) Carbon-fluorine coupling (in 13C) for d-Y6 and d-L8-BO should be included in NMR data.

Reply: We thank the reviewer for this important comment. We have added the enlarged ^{13}C NMR spectrum of *d*-Y6 (between 150 and 160 ppm) to the inset of **Supplementary Fig.3**. The presence of C-F coupling is evidenced by the doublet at δ 155.64 (d, *J*=16.2 Hz), 153 (dd, *J*=14.8, 7.3 Hz).

Supplementary Fig.3 has been modified as shown below.

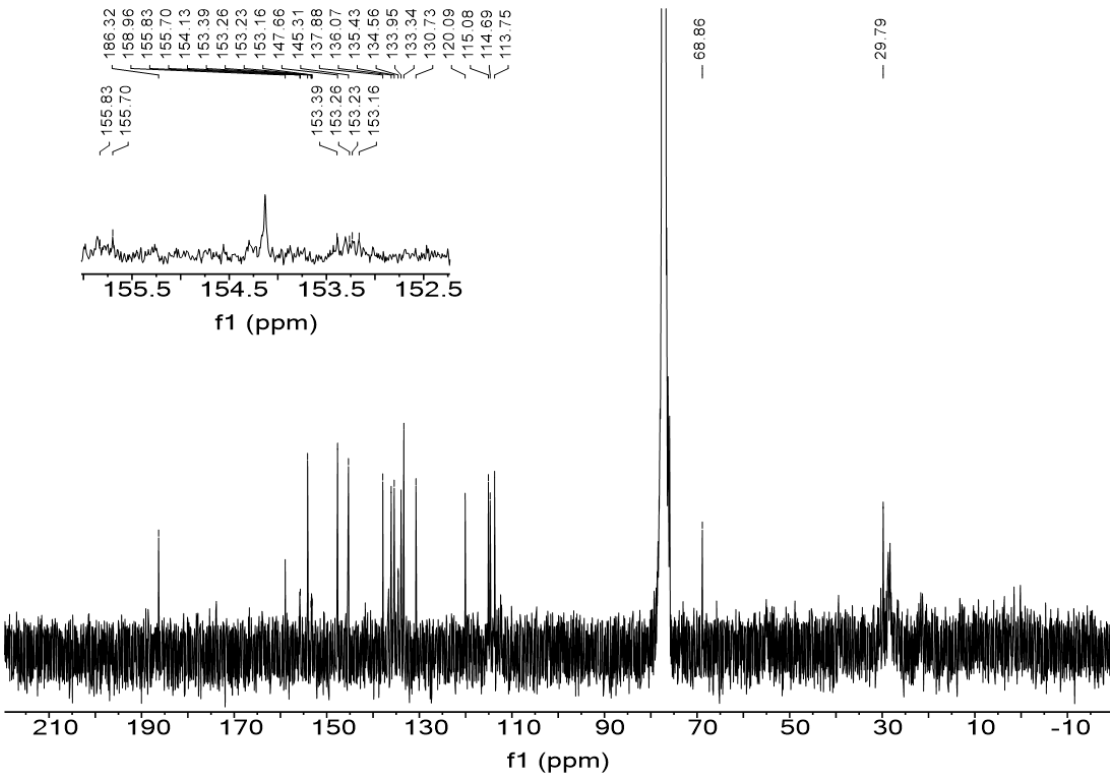

Supplementary Fig. 3 ^{13}C NMR spectrum of *d*-Y6. The inset is the enlarged spectrum

between 152 and 156 ppm to highlight the presence of C-F coupling.

We have also added the following comments in Supporting Information.

^{13}C NMR (100 MHz, Chloroform-*d*) δ 186.3, 159.0, 154.1, 147.7, 145.3, 137.9, 136.1, 135.4, 134.6, 134.0, 133.3, 130.7, 120.1, 115.1, 114.7, 113.7, 68.9, 29.8. The presence of C-F coupling is evidenced by the doublet at δ 155.64 (d, *J*=16.2 Hz), 153 (dd, *J*=14.8, 7.3 Hz).